**Distribution Agreement**

In presenting this thesis as a partial fulfillment of the requirements for a degree from Emory University, I hereby grant to Emory University and its agents the non-exclusive license to archive, make accessible, and display my thesis in whole or in part in all forms of media, now or hereafter now, including display on the World Wide Web. I understand that I may select some access restrictions as part of the online submission of this thesis. I retain all ownership rights to the copyright of the thesis. I also retain the right to use in future works (such as articles or books) all or part of this thesis.

Xi Jiang 04/12/2013

# Exploring the Relationship of Abasic Sites to Reactive Oxygen Species Generation in a Yeast Model System

by

Xi Jiang

Paul Doetsch

Adviser

Department of Biology

Paul Doetsch

Adviser

William Kelly

Committee Member

Yoke Wah Kow

Committee Member

Gregg Orloff

Committee Member

04/12/2013

# Exploring the Relationship of Abasic Sites to Reactive Oxygen Species Generation in a Yeast Model System

by

Xi Jiang

Paul Doetsch

Adviser

An abstract of

a thesis submitted to the Faculty of Emory College of Arts and Sciences

of Emory University in partial fulfillment

of the requirements of the degree of

Bachelor of Sciences with Honors

Department of Biology

04/12/2013

Abstract

Exploring the Relationship of Abasic Sites to Reactive Oxygen Species Generation in a Yeast Model System

By Xi Jiang

Abasic (AP) sites, the common intermediate in single-base DNA damage/repair, are among the most frequently formed lesions in DNA. DNA damage accumulation may lead to mutations deleterious to health, contributing to carcinogenesis, neurodegeneration, and aging. In *Saccharomyces cerevisiae* (budding yeast), the amount of intracellular reactive oxygen species (ROS) increases when DNA damage is chemically induced. Base excision repair (BER) and nucleotide excision repair (NER) pathways are crucial in DNA repair (including AP site removal), and cells with deficient BER show an increase in both spontaneous DNA damage accumulation and intracellular ROS level. We hypothesize that, as an abundant common intermediate, abasic site may be responsible for originating genotoxic stress signaling via ROS generation. The yeast DNA glycosylase Ung1 creates abasic sites by uracil excision. Knockout of Ung1 should prevent uracil (incorporated into DNA/spawned from cytosine deamination) from being excised, thereby reducing the level of abasic sites present. If the level of abasic sites positively correlates with ROS generation, Ung1 knockout should lead to a reduction of mutation frequency due to abasic site's mutagenic nature, alongside a decrease in intracellular ROS level. Cells that are completely deficient in BER, as well as those impaired in both BER and NER, showed such correspondence, providing evidence suggesting that abasic sites are responsible for DNA-damage-induced ROS response. To further determine the exact source of ROS generation, we postulate that the ROS response may be compartmentalized, since many enzymes in the BER pathway (including Ung1) are capable of localizing to either the nucleus or mitochondria upon induced DNA damage. Ung1 mutants that selectively localize to either the nucleus or mitochondria were created, and the ROS generation observed was similar to that of Ung1 knockout, indicating that dynamic localization may be required for the ROS response to be maintained.

# Exploring the Relationship of Abasic Sites to Reactive Oxygen Species Generation in a Yeast Model System

by

Xi Jiang

Paul Doetsch

Adviser

A thesis submitted to the Faculty of Emory College of Arts and Sciences

of Emory University in partial fulfillment

of the requirements of the degree of

Bachelor of Sciences with Honors

Department of Biology

2013

Acknowledgements

I would like to acknowledge Nick Bauer, whose patience and vigor made him a valuable mentor of mine, Dr. Paul Doetsch, my research advisor, Dr. Natalya Degtyareva, who served as my unofficial advisor, and all the members of the Doetsch Lab (past and present) for their assistance and care. Without their help, this project could not have been done.

Table of Contents

## Background

Deoxyribonucleic acid (DNA) can experience damage from many sources, most commonly reactive oxygen species (ROS) and ionizing radiation (*11*). DNA damage accumulation, in turn, affects human health deleteriously through mutagenesis and cytotoxic blockage of transcription/replication (*2*). Single base lesions are among the most abundant forms of DNA damage, which includes methylation, oxidation, and deamination of normal DNA bases; misincorporation of damaged nucleotides into DNA during replication, especially deoxyuridine, may also introduce lesions (*2*, *3*). In humans and many other organisms, including the budding yeast *Saccharomyces cerevisiae*, BER and nucleotide excision repair (NER) are the major pathways responsible for the repair of all aforementioned single base damages (*3*,*13*). Evidence that these pathways are important to human health exists: deficiency in BER has been linked to colorectal cancer development (*14*), while inherited defect in NER leads to earlier onset of xeroderma pigmentosum (*15*).

Reactive oxygen species (ROS), such as superoxide, hydroxyl radical and hydrogen peroxide, damage cellular macromolecules (including DNA) directly, mediating deleterious effects that contribute to human degenerative conditions (*1*). ROS may arise from both exogenous and endogenous sources, the former associated with environmental stimuli such as UV radiation/chemotherapeutic agents, and the latter with cellular metabolism involving oxygen, as seen in the mitochondria (*16*). While enzymes that scavenge free radicals and neutralize ROS exist to prevent oxidative damage (*16*), DNA repair pathways are capable of repairing oxidative lesions that do occur. The amount of DNA damage may accumulate, however, to the point where the cellular repair capacity may be exceeded, leading to mutagenic bypass of lesions in favor of

replication (i.e. translesion synthesis) and, in the case of multicellular organisms, programmed cell death (17).

Abasic (apurinic/apyrimidinic, or AP) sites, the most common DNA lesions *in vivo* (*13*), may arise endogenously from hydrolysis or, in the course of the base excision repair (BER) process, from the removal of damaged single bases by DNA glycosylases (*2*). The spontaneous depurination rate in double-stranded DNA is approximately 10,000 purines per human cell per day (*2*), and a normal human liver cell possess a steady-state level of around 50,000 AP sites (*12*). AP sites are cytotoxic due to blockage/inactivation of DNA polymerases (*39*), and are mutagenic when DNA/RNA polymerases bypass them with insertion of inappropriate bases (*2, 4*). In the BER pathway, which is highly conserved between yeast (*S. Cerevisiae*) and humans, repair of AP sites is initiated by an AP endonuclease or bifunctional glycosylases with lyase activity (*1, 2*) by cleaving the DNA backbone, either on the 5' side of the AP site by AP endonuclease or on the 3' side by AP lyase (*2*). This is followed by re-formation of 3' hydroxyl/5' phosphate at DNA strand break, DNA polymerase's replacement of excised bases, and DNA ligation (*2, 9*). While there have been attempts to elucidate the involvement of BER in response to oxidative stress within a yeast model system, the regulation of BER upon DNA damage induction is not yet well-understood in terms of enzyme mobilization and localization (*5*).

Previous studies have observed a correlation between the production of ROS and DNA damage; for example, ROS levels have been reported to increase in a dose-dependent fashion following yeast cells' exposure to the DNA-alkylating agent MMS or ultraviolet light (*1*). While ROS can be deleterious to cells, they may also function as stress-induced signaling molecules, participating in cells' responses, e.g. activation of DNA repair mechanisms and transcription factors as well as other cell operational systems (*18*). It has been postulated that DNA damage in

some way signals enhancement of cellular oxidase activities (*1*), which produce a higher level of ROS for initiating DNA damage responses, including activation of DNA repair pathways, such as BER (*Figure 1*). As abasic sites are the common intermediates in DNA base damage/repair, we hypothesize that they may be a critical signal in the ROS response to DNA damage, where the generation of ROS signals by cellular oxidases (e.g. NADPH) (*23*) may recruit enzymes involved in repair pathways to the site of damage (*22*).

The first step in establishing the role of abasic sites, then, is to gauge the scarcely investigated correlation between level of abasic sites and the level of ROS generation, necessitating the quantification of abasic sites and the measurement of endogenous ROS. While many different ROS species exist and are reported to be involved in signaling (*18*), it is recognized that the NADPH oxidase complex, which is present in the mitochondria and catalyzes the production of superoxide ($O_2^-$), is a major source of ROS (*23*). Further reduction of superoxide produces hydrogen peroxide ($H_2O_2$), and leads to subsequent formation of hydroxyl radicals (•OH) (*18*). Measurement of intracellular superoxide levels, in turn, should be a representative way of determining whole-cell ROS levels. Fluorescence-based flow cytometry, the analysis of light scatter and cellular fluorescence in a fluidic cell suspension presented to laser-based detectors, is a well-established technique for gathering data from cell populations (*24*, *25*), and has been utilized in gauging redox status in both yeast and mammalian cells (*25, 26*). Dihydroethidium (DHEt), a fluorescent dye specific to superoxide, has been utilized in yeast and employed in flow cytometry (*1, 27*). To measure endogenous ROS using flow cytometry with dihydroethidium should therefore be a suitable choice.

While several methods for abasic site quantifications exist, such as oligomeric DNA probes, mass spectrometry, and positron-emission tomography (*28-30*), the high requirement for

equipment and cost restricts their use. Comparatively more cost-efficient assessment of AP sites is often achieved in vitro based on relative chemiluminescence using an aldehyde reactive probe (ARP) (*30-32*). ARP (N-(Aminooxyacetyl)-N'-biotinylhydrazine) covalently binds to AP sites in open-ring aldehyde forms (*32*) and labels them with biotin, a moiety with high affinity to streptavidin, allowing the number of AP sites to be quantified via a streptavidin-horseradish peroxidase colorimetric assay (*31*). Alternatively, the introduction of repair deficiency (especially in BER) may alter the cell's AP site generation and repair capacity, thereby modulating the level of abasic sites present. In yeast, the monofunctional, evolutionarily conserved DNA glycosylase Ung1 removes uracil from the genome (*19*). Ung1 knockout should prevent uracil (incorporated into DNA/generated from cytosine deamination) from being excised, thereby reducing the level of abasic sites that accumulates. Therefore, by introducing Ung1 knockout, the effect of altered abasic site level on ROS generation may be observed. In yeast, cellular resistance to canavanine (an arginine analog that impairs protein synthesis) requires a loss of function mutation in the gene coding for arginine permease (*34*). Aside from direct quantification, the level of abasic sites (which may account for much of DNA damage accumulation in BER deficient backgrounds) can be indirectly assessed via canavanine-based spontaneous mutation frequency assays, the results of which denote level of DNA damage (*33, 34*).

Unlike its human homologs, which are largely restricted to either the nucleus or the mitochondria, the yeast Ung1 is found in both compartments (*3, 5, 19-21*), suggesting that it may be capable of dynamic localization upon DNA damage (*1*). In addition, the sequence of Ung1 contains a putative mitochondria targeting sequence (MTS) and nuclear localization sequences (NLS), and mutations in said sequences abolish the localization of Ung1 to either compartment

selectively, as observed through fluorescence microscopy of GFP-attached Ung1 mutants (N. Bauer, Doetsch Lab, unpublished). It is known that another enzyme in the BER pathway, Ntg1, engages in dynamic localization, which is hypothesized to be a major regulatory mechanism in response to oxidative damage (*5, 22*). As the regulation of enzymes involved in BER pathway potentially requires signaling in a compartment-specific manner, the source of observed ROS response to DNA damage may be compartment-specific as well. Therefore, Ung1 mutants that localizes exclusively to one compartment will be informative on the origin of ROS signal as a part of genotoxic stress response.

This study investigates the hypothesis that abasic sites are an important source of ROS generation in genotoxic stress signaling and, consequently, that abasic site levels will positively correlate with intracellular ROS. The expectation is that, in an Ung1 knockout, mutation frequency will be reduced due to abasic site's mutagenic nature, alongside a corresponding decrease in ROS level. We also postulated that the source of ROS generation may be compartment-specific, whereby repair-deficient yeast strains expressing Ung1 mutants incapable of dynamic localization may display reduced whole-cell ROS level.

## Materials and Methods

### Strains, Media, and Growth Conditions

The haploid *S. cerevisiae* strains used in this study are derived from hDNP119, a diploid strain heterozygous in key enzymes of BER and NER (*Table 1*), by asci dissection and selection via respective markers. Yeast cells were cultured on YPD media (1% yeast extract, 2% peptone, 2% dextrose, and 2% agar for plates) at 30 ℃, or on SD-complete media (5g ammonium sulfate, 1.7 g/L yeast nitrogen base, 1.4 g/L amino acid-nucleotide mix, 2% dextrose, and 2% agar) for

pAC4 transformants. Liquid YPD media was inoculated with yeast cells and grown at 30 ℃ for ~48 h (with 1:100 dilution after one night for ROS measurement/ARP assay, and with 1:100 dilution after ~48 h followed by 6 h incubation for spontaneous mutagenesis assay). Cell growth was determined by OD600 value from spectrophotometer (around 0.3-0.6 for mid-log phase).

Ung1 Localization Mutant-containing Plasmids and Strain Construction

The localization mutants (*Figure 2*) were generated via site-directed mutagenesis on 2μ plasmids with GFP for visualization, whereby their impaired localization was confirmed (N. Bauer, unpublished work). To reduce the level of expression, the Ung1 mutants were transferred to yeast *CEN*-bearing plasmids (pAC4) of pRS316 (*8*) backbone. pAC4 plasmids were also constructed for the expression of wildtype Ung1, which may be introduced back to knockouts for phenotype rescue. A well-characterized and conserved catalytic mutant (carrying one aspartate to asparagine substitution at the active site) (*3*) was also incorporated as control. (*Figure 2*)

MMS Treatment

Methyl methanesulfonate (MMS), a DNA alkylating agent known to induce abasic site production (*1*), was employed for ROS measurement/ARP assay. Yeast cells were grown as previously stated before treatment. 0 mM and 25 mM MMS were employed to treat 5ml saturated cultures of hDNP119-derived WT, $BER^-$ and $BER^-/NER^-$ strains (without Ung1 knockout). The concentrations chosen were based on survival data for greater than 50% survival and significant (up to 1.8 fold) differences in ROS levels measured (*1, 5*).

After treatment (1 h, 30 ℃), each culture was divided into two, one set for DNA purification and subsequent abasic site quantification, and the other for ROS measurement via flow cytometry.

DNA Purification and Damage Quantification

Purification of DNA in MMS-treated samples was performed using kit and protocol from EPICENTRE® Biotechnologies (zymolyase-based lysis and ethanol/isopropanol precipitation). The aldehyde reactive probe (ARP; (*N*-(aminooxyacetyl)-*N*′-biotinylhydrazine), which covalently binds to AP sites and labels them with biotin, allowing the number of AP sites to be quantified via a streptavidin-HRP colorimetric assay (*31*). To control for possible background noise of ARP assay (e.g. ARP binding to unpurified protein/RNA remains in genomic DNA samples), DNA from one sample for each strain was treated with 0.1 M $NaBH_4$ at room temperature for 2 h to reduce all aldehydes to hydroxyls, which do not react with ARP. The samples were then neutralized with 0.05 M HCl and dialyzed against 10 mM sodium phosphate buffer, pH 7.5.

Abasic site abundance was assessed using DNA damage quantification kit (BioVision). The DNA samples previously obtained (including $NaBH_4$ treated) were tagged by ARP, bound on microplate, and labeled with HRP-Streptavidin. O.D. values were measured for each sample at 650 nm and plotted against a standard curve prepared with the quantification kit.

Reactive Oxygen Species Level Measurement and Flow Cytometry

The fluorescent probes dihydroethidium (DHEt) and MitoSox Red were planned to be employed to detect whole-cell superoxide and mitochondrial superoxide levels, respectively (*1*). Dyes that detect other species, such as Amplex Red (APR, specific to H2O2) and 2-[6-(4′-hydroxy) phenoxy-3H-xanthen-3-on-9-yl] benzoic acid (HPF, specific to hydroxyl radical) (*1*), were conceived for use, but attempts with APR were unsuccessful due to instrumentation constraints (laser wavelength of the cytometer not optimal for dye excitation). Following probe

addition, cells were incubated at 30 ℃ for 2 h. Cells were then washed twice with H2O, resuspended in phosphate-buffered saline (PBS), and assessed for fluorescence intensity employing a BD LSR II flow cytometer (BD Biosciences). 10,000 cells were evaluated for fluorescence intensity independently in every sample.

Spontaneous Mutagenesis Assays

Detection of mutations inactivating the arginine permease gene (*CAN*$^r$ mutations) through canavanine-containing selective media was employed to assess the spontaneous mutation frequencies of strains with and without Ung1 knockout (*7*), using three to six independent cultures per strain per experiment.

Data Analysis

Flow cytometry data was analyzed using FlowJo (*Figure 3*), where geometric means were obtained from the approximately lognormal distributions (*Figure 4*) as representative of the sample populations (*10*). Analysis of variance (ANOVA, Stata 12) and Student's *t*-test (significance at $\alpha = 0.05$ and $p = 0.05$, respectively) were performed to assess the effect of Ung1 knockout and mutants. The correlation between spontaneous mutation frequencies and background ROS levels was examined by linear regression.

## Results

Heating DNA adversely affects the ARP assay

ARP assay/ROS measurements were conducted for DSC226 and DSC499 (wildtype and *ung1Δ*, respectively), with 0 mM/25 mM MMS treatment for each strain, as well as in wildtype and BER$^-$ hDNP119 isolates (*Table 1*). Despite repeated trials, the ARP assay did not generate

consistent, repeatable results from yeast DNA, although methods that do not involve heating have not been tested in conjunction with the ARP assay. Heated pre-treated calf thymus standard DNA displayed reduced standard curve slope, potentially reflecting a reduction in ARP-binding lesions (*Figure 5*). High OD value measured across all samples were observed in hDNP119 isolates, including $NaBH_4$-treated ones and regardless of MMS treatment status, suggesting that the elevated background signal was not solely due to presence of abasic sites (*Table 2*). Without reliable ARP data, ROS measurements cannot be correlated to abasic site levels reasonably, and AP site quantification by ARP was not pursued further.

Spontaneous mutation frequency reductions observed in Ung1 knockouts

Since the problematic ARP assay did not allow direct quantification of abasic sites, spontaneous mutation frequencies were measured instead of abasic site levels as an indicator of mutagenic DNA damage, including abasic sites (since abasic sites are both abundant and mutagenic, their contribution to mutation rates likely predominates). As with the background ROS measurements/ARP assays, mutagenesis assays employed yeast strains known to have different AP site repair capacities and with/without Ung1 knockout (*Table 1*, *Figure 11*). Strains impaired in $BER^-$ and/or $NER^-$ showed elevation in mutagenesis over WT, and the degree of elevation is in correspondence to the extent of repair pathway blockage ($BER^-/NER^-$ > $BER^-$ > *apn1Δ*) and, by extension, the level of abasic sites present. (*Figure 6*) This observation is consistent with the expectation that abasic sites should be a major source of mutation. A decrease in mutation frequency was observed in association with Ung1 knockout for the *apn1Δ*, $BER^-$, and $BER^-/NER^-$—which serves as a DNA damage level/ROS generation positive control—isolates. In contrast, an elevation was observed in the otherwise wildtype *ung1Δ* strain. The $NER^-$ deficient isolates, intended as negative control, displayed no change in mutation frequency

associated with Ung1 knockout. (*Figure 6*) All aforementioned observations were shown to be significant via ANOVA (*Table 3*, top).

ROS production decreases in BER$^-$ and BER$^-$/NER$^-$ background with Ung1 knockout

Measurement of ROS production via DHEt revealed that, accompanying the reductions of mutation frequency observed, BER$^-$/NER$^-$ and BER$^-$ only strains have lower intracellular ROS levels with Ung1 knockout (*Figure 7*). The flow cytometry results for *apn1Δ, ung1Δ*, however, vary between isolates, one of which shows an elevation instead over the corresponding UNG1 strain. This elevation was not remedied by re-introduction of wildtype Ung1 (*Figure 9*). No apparent effect is observed with Ung1 knockout in the other partial BER deficient background, which lacks bifunctional glycosylases Ntg1 and Ntg2 (*Figure 7*). The NER$^-$ control, as expected, shows no apparent change in ROS associated with *ung1Δ*. In the otherwise wildtype *ung1Δ*, the ROS level is comparable to that of its *UNG1* counterpart. Given that results from *apn1Δ* varied greatly between isolates and that no mutation frequency data for *ntg1Δ, ntg2Δ* was available, ANOVA was performed for ROS production with BER, NER and *UNG1* as predicator variables (*Table 3*, bottom). Most interactive effects were significant, with the exceptions of NER alone and BER/NER/*UNG1*, in accordance to our expectation that NER plays a lesser (i.e. backup) role in abasic site repair.

ROS generation correlates with mutation frequency

In BER$^-$ and BER$^-$/NER$^-$ backgrounds, isolates with Ung1 knockout possess both lowered mutation frequency and decreased ROS production compared to their Ung1 wildtype counterparts., and a significant positive correlation was observed ($R^2 = 0.78$, greater than 0.5) (*Figure 8*).

Ung1 localization mutants display ROS levels similar to an Ung1 knockout mutant

In yeast, it has been shown that Ung1 localizes in a compartment-specific manner (*40*), and its nuclear localization sequence (NLS) and mitochondrial targeting sequence (MTS) have been putatively identified. Reintroducing wildtype Ung1 elevated superoxide level in BER$^-$/NER$^-$, *ung1Δ* background, whereas expression of the Ung1 catalytic mutant did not (*Figure 10*). The Ung1 localization mutant-carrying isolates did not seem to differ from their Ung1 knockout counterpart in terms of ROS generation.

## Discussion

The objective of this study was to evaluate the importance of AP sites as a component for generating reactive oxygen species (ROS) in genotoxic stress signaling. For this purpose, the correlation between, as well as the compartmentalization of, abasic site and intracellular ROS were investigated in a yeast model system. Strains deficient in BER and/or NER pathways were constructed to yield changes in level of DNA damage associated with AP sites (*Table 1*, *Figure 11*), and in localization of Ung1 to the nucleus or mitochondria (the DNA-containing compartments). The hypotheses tested are as follows: abasic site levels will positively correlate with intracellular ROS, as well as mutation frequency; the production of ROS as DNA-damage stress response may be compartmentalized, leading to reduced whole-cell ROS level in strains expressing Ung1 localization mutants. Evidence supporting the former was obtained through correlation of mutation frequency and ROS level, while the latter was not supported by the flow cytometry data, indicating that dynamic localization may be required to maintain ROS generation as part of the DNA damage stress response.

High background signal in the ARP assay limits its application in yeast

While the ARP assay was expected to establish a relationship between higher abasic site levels with increased MMS exposure doses employed on WT strains, a lack of such correlation may suggest human error, lower than expected efficiency of ARP or less than optimal conditions of the kit. While the efficiency of $NaBH_4$ treatment, which should eliminate all aldehydes present and provide negative control samples, was at question due to high background OD values observed (*Table 2*), inefficient elimination of AP sites in controls cannot explain the similarity of OD values in both 0 mM (control) and 25 mM MMS-treated samples. The most likely explanation seems to be the reduced affinity of the probe due to the heating required (to disrupt the yeast cell wall) in genomic DNA extraction (*35*), as the data from Figure 5 suggests, since the DNA extraction method employed required heating at 65 ℃, a step not required with ARP applications in bacteria and mammalian cells (*32, 35*). A lowered binding efficiency of ARP at abasic sites for heated samples, possibly due to conformational alterations and heat-induced degradations (*36*), has been proposed earlier (*35*).

Mutation frequency/superoxide level correlation supports a role for AP sites in ROS generation

Since knockout of Ung1 should prevent uracil excision, the level of abasic sites present should be reduced under $BER^-$ impaired backgrounds (for WT, the repair may have been robust enough that not much difference could be observed). A clear reduction in mutation frequencies with *ung1Δ* in *apn1Δ*, $BER^-$ and $BER^-/NER^-$ backgrounds was observed, as expected from the high mutagenic potential of AP sites (*2, 4*). Given the elevated presence of uracil in DNA due to Ung1 knockout and the reduction in mutation frequency for *ung1Δ* despite said presence, the importance of abasic sites in mutagenesis is likely greater than that of uracil within DNA when

the BER pathways are compromised. The lowering of background ROS for BER$^-$ and BER$^-$ /NER$^-$ with *ung1Δ* corresponded to the observed reduction in mutation frequency and lower abasic site level inferred from genetic background, providing evidence that abasic sites may be responsible for DNA-damage-induced ROS The importance of AP sites in genotoxic stress signaling via ROS is thus supported, and warrants further investigation.

In the *apn1Δ* background, the relationship between *apn1Δ* and *apn1Δ*, *ung1Δ* isolates is not consistent, with one *ung1Δ* isolate showing an elevation in ROS over its *UNG1* counterpart but not the other (*Figure 7*). Transformed with pAC4-*UNG1*-GFP did not reduce the ROS level in *apn1Δ*, *ung1Δ* to that of the *apn1Δ* only, suggesting that the elevation observed was not solely due to Ung1 knockout. Employing a third *apn1Δ*, *ung1Δ* isolate confirmed that *ung1Δ* indeed has little effect alongside *apn1Δ*, and that the elevation in ROS seen in the first *apn1Δ*, *ung1Δ* isolate is likely not dependent on absence of Ung1. While an independent role for NER in ROS generation was suspected, inspection of NER- isolates detected no significant difference in mutation frequency or ROS levels alongside *ung1Δ*, as to be expected for a pathway not primarily involved in repair of abasic sites.

Further trials are needed for validation of the current results, especially for newly acquired isolates, as the low number of biological replicates for each mutant isolate may have contributed to the variability of the data collected so far. Transformation with pAC4-*UNG1* in the BER-/NER-, ung1Δ increased superoxide level closer to that of its *UNG1* counterpart, with the implication that changes in ROS generation are dependent on Ung1 knockout and, as is likely the case for a monofunctional glycosylase, on the abundance of abasic sites. From the current set of data, it appears that partial BER deficiency may not be enough to push the cells into an oxidative stress state characterized by chronic elevation of ROS, as previously observed with

chemically induced DNA damage (*1*). Spontaneous mutation frequency data from *ntg1Δ*, *ntg2Δ* background may further support this notion, but no reliable data has been obtained due to culture contamination.

Dynamic localization of Ung1 may be involved in DNA damage-induced ROS response

It was expected that one of the localization mutants would display a greater level of intracellular ROS than the other, thereby denoting the primary source of ROS generation due to the presence of abasic sites. However, whole-cell superoxide measurement results from flow cytometry suggested that both NLS and MTS mutants of Ung1 did not significantly differ from the $BER^-/NER^-$, *ung1Δ* background with respect to ROS generation. It may be premature to claim that unimpaired dynamic localization of Ung1 is necessary for the production of ROS signal following AP site creation, given the small sample pool and measurement reliance on a single ROS species over the entire cell. Nevertheless, the absence of ROS elevation remains puzzling. If dynamic localization is indeed involved in ROS generation, it may not be sufficient by itself, as the catalytic mutant-carrying isolate showed no elevation in ROS comparable to that of UNG1 wildtype (either endogenous or back-transformed with pAC4).

In summary, this project demonstrated that the lowering of background ROS for $BER^-$ and $BER^-/NER^-$ backgrounds with *ung1Δ* corresponded to the observed reduction in mutation frequency and inferred lower abasic site level, providing evidence that abasic sites may be responsible for DNA-damage-induced ROS response. Partial BER deficiency, such as knockout of Ntg1 and Ntg2, seems insufficient to elevate cellular ROS to consistently elevated levels (*Figure 7*). Dynamic localization of Ung1 may be involved in ROS signal production after DNA damage, or it may be required to maintain ROS level as a stress response. In addition, the

importance of abasic sites in mutagenesis is shown to be likely greater than that of uracil within DNA, as clear reductions in mutation frequencies with *ung1Δ* in BER$^-$ and BER$^-$/NER$^-$ backgrounds indicated.

Future Directions

Ung1 is a specific DNA glycosylase with no other functions, and knockout of other/multiple glycosylases, while potentially lowering abasic site levels, may cause undue influences in terms of mutagenesis and ROS generation: for instance, Mag1, a 3-methyladenine DNA glycosylase, has been implicated in homologous recombination susceptibility (*37*); and Ogg1, the 8-oxoguanine glycosylase, causes single strand breaks with its lyase activity. Still, it is desirable to obtain a finer control over the amount of abasic sites present, and this may be achieved either through employing a more reliable method of direct abasic site quantification or utilizing inducible, graded expression of monofunctional glycosylases, such as Ung1. Informative ROS probes specific to species other than superoxide may also be desirable for a more thorough investigation of ROS response to DNA damage.

Among the aforementioned leads, titratable expression of glycoslyase has already been attempted. Single amino acid substitutions of human uracil-DNA glycosylase (UDG) produce mutagenic, selective DNA glycosylases, CDG and TDG, which release normal pyrimidines cytosine and thymine, respectively (*38*). CDG and TDG have been successfully introduced via plasmid and expressed in yeast cells (*35*). Because CDG and TDG possess no other known enzymatic activity and because their mutator effects are much greater in a BER impaired background, the mutagenic effect of these enzymes is most likely due to the formation of AP sites (*35*). To provide greater control over the generation of abasic sites, strains with *GAL1*-

promoted mutant human UDG that remove normal cytosine bases have been constructed, but unsuccessful insertion of a selectable marker prevented further examination for mutation frequency/ROS under different levels of glycosylase expression (data not shown). Once the marker is in place, the CDG construct should provide a relative estimate for abasic site levels present, while avoiding complications that may arise with knockout of functionally complex glycosylases.

# Figures

Figure 1

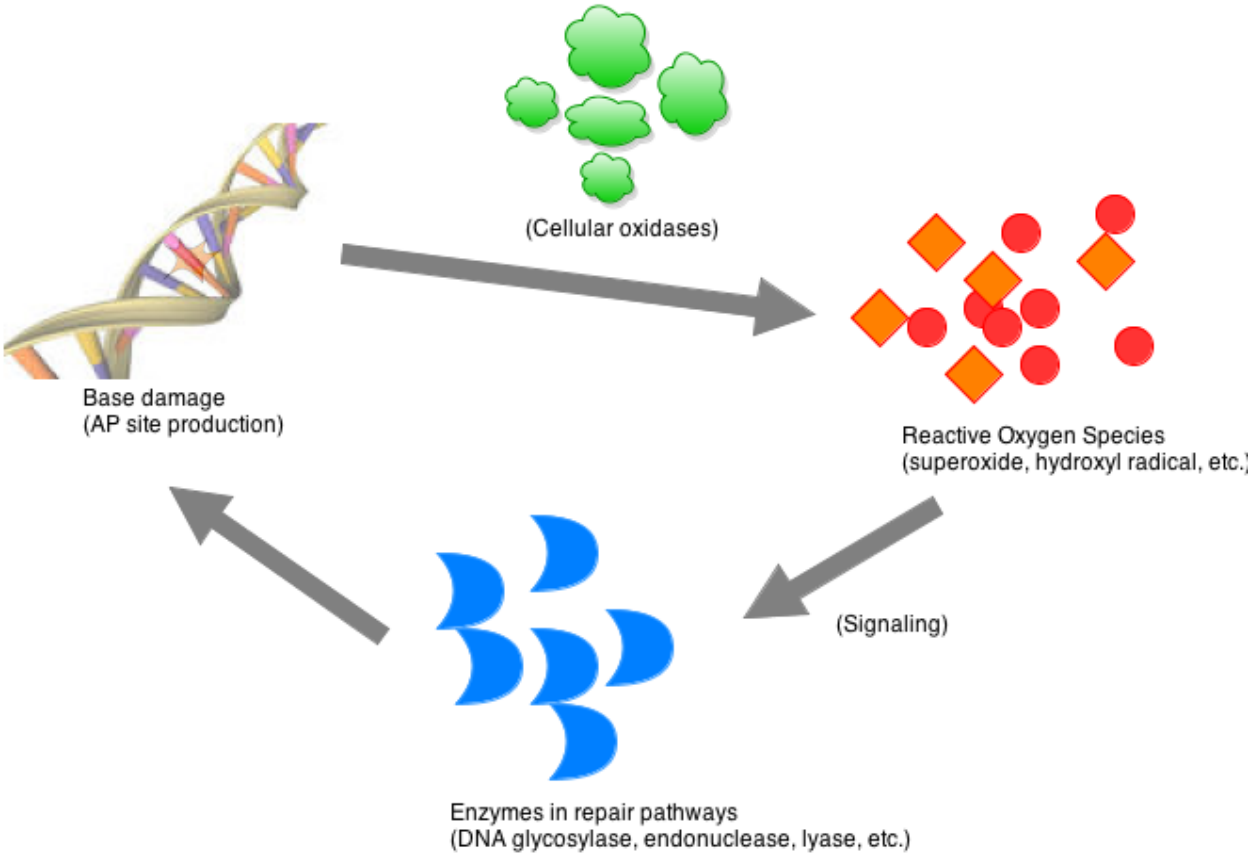

Figure 2

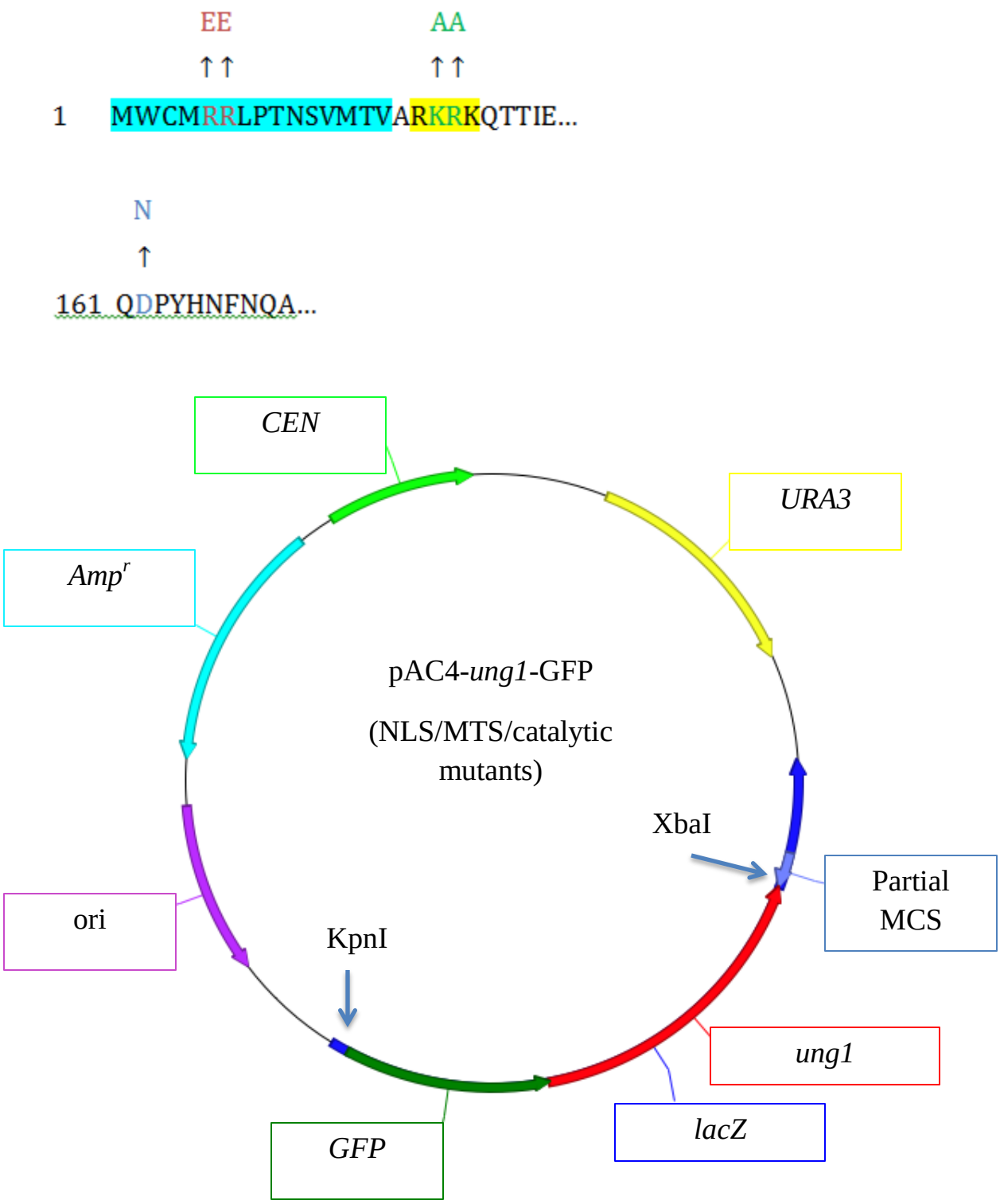
EE
AA
1 MWCMRRLPTNSVMTVARKRKQTTIE...
N
161 QDPYHNFNQA...
CEN
URA3
Amp^r
pAC4-ung1-GFP
(NLS/MTS/catalytic mutants)
XbaI
Partial MCS
ori
KpnI
ung1
lacZ
GFP

Figure 3

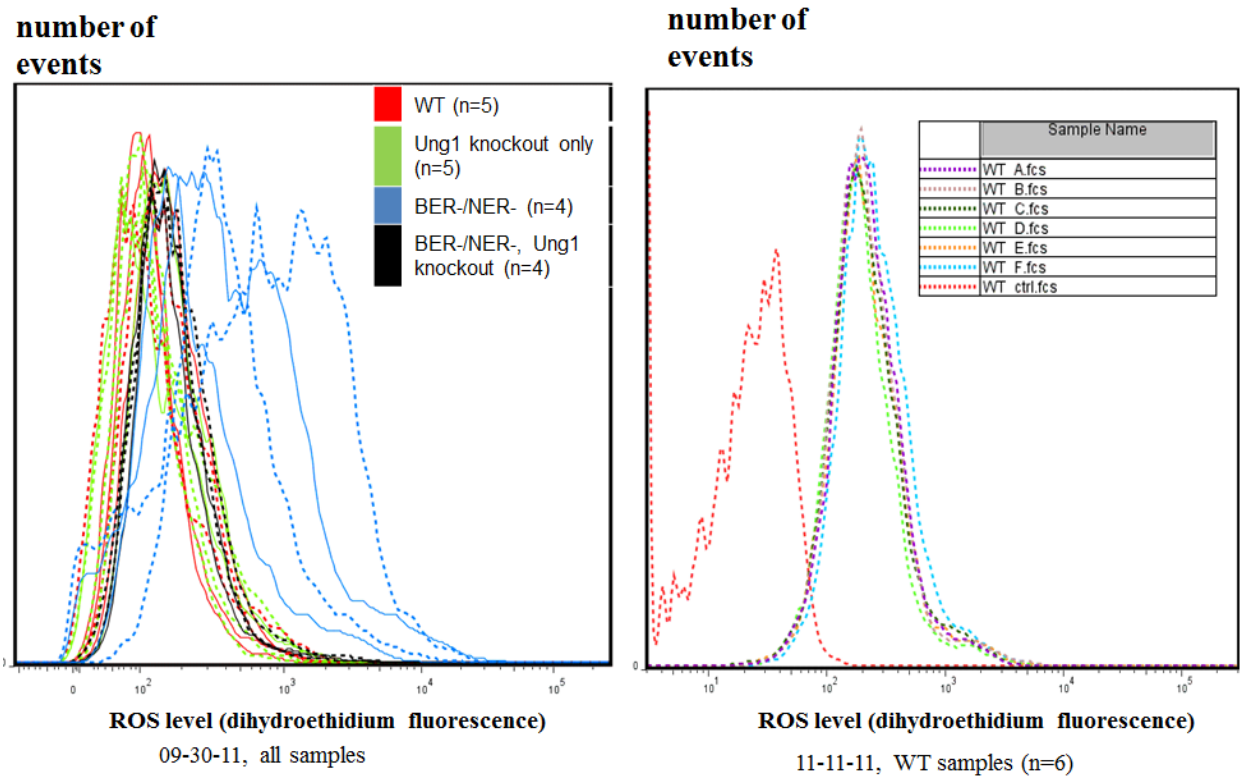
number of events
WT (n=5)
Ung1 knockout only (n=5)
BER-/NER- (n=4)
BER-/NER-, Ung1 knockout (n=4)
ROS level (dihydroethidium fluorescence)
09-30-11, all samples
number of events
Sample Name
WT A.fcs
WT B.fcs
WT C.fcs
WT D.fcs
WT E.fcs
WT F.fcs
WT ctrl.fcs
ROS level (dihydroethidium fluorescence)
11-11-11, WT samples (n=6)

Figure 4

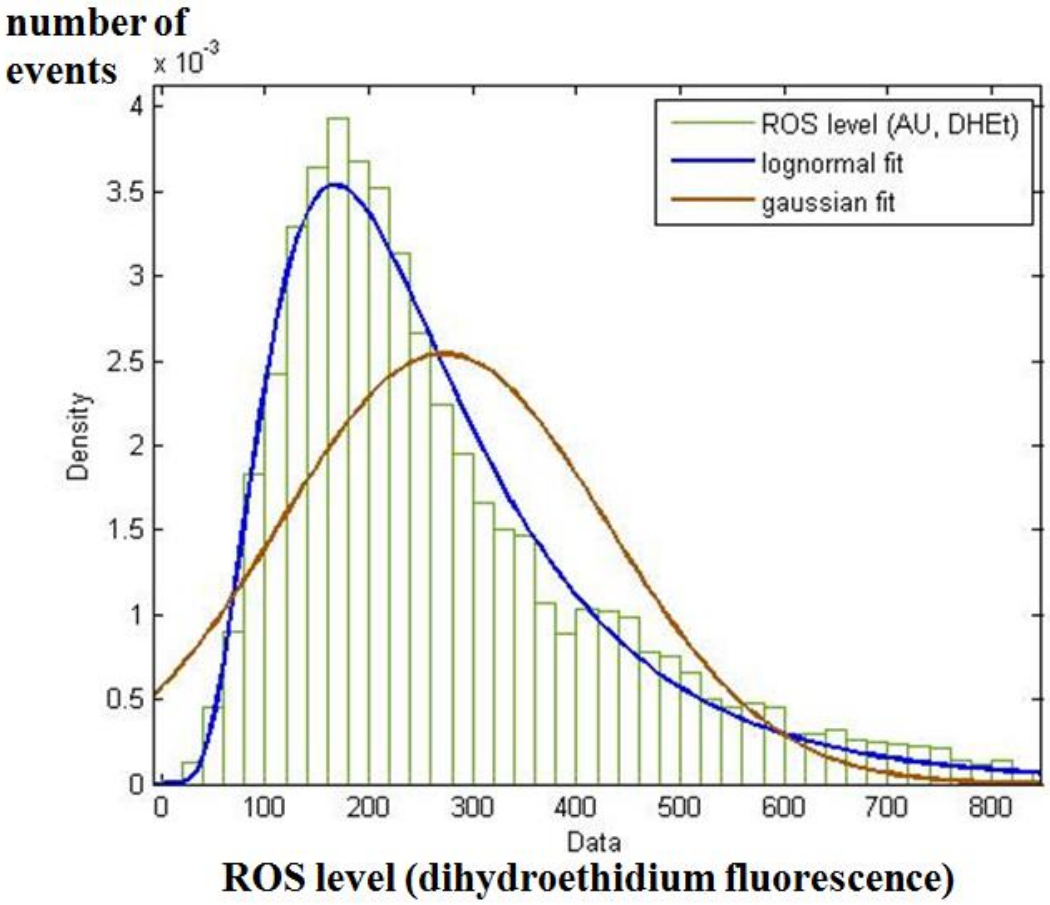
number of events
x 10^-3
4
3.5
3
2.5
2
1.5
1
0.5
0
Density
0
100
200
300
400
500
600
700
800
Data
ROS level (AU, DHEt)
lognormal fit
gaussian fit
ROS level (dihydroethidium fluorescence)

Figure 5

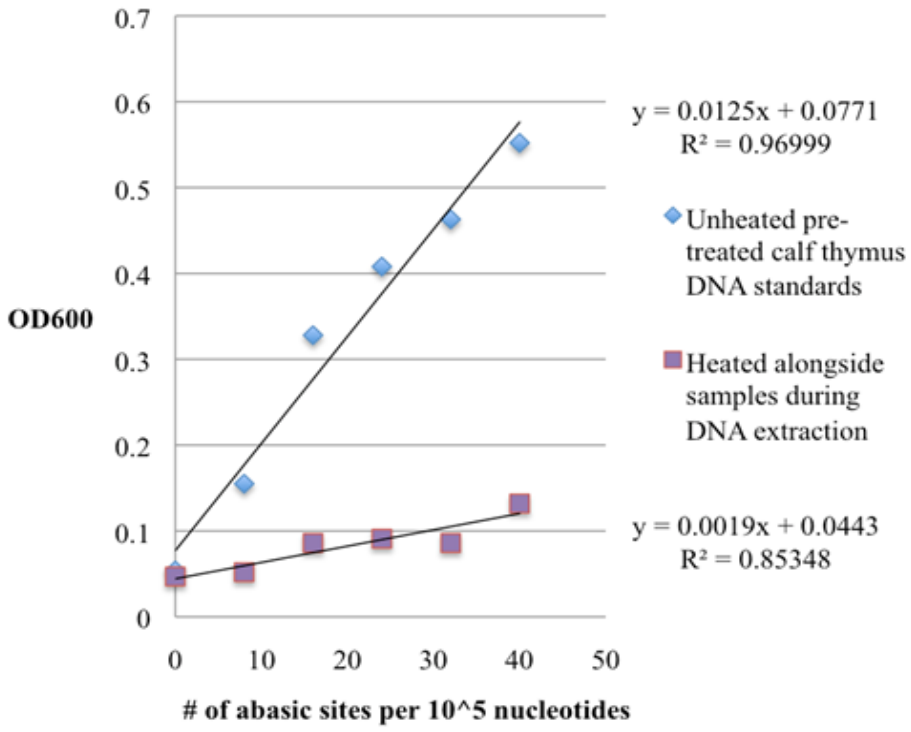
0.7
0.6
0.5
0.4
0.3
0.2
0.1
0
OD600
0
10
20
30
40
50
# of abasic sites per 10^5 nucleotides
y = 0.0125x + 0.0771
R² = 0.96999
Unheated pre-treated calf thymus DNA standards
Heated alongside samples during DNA extraction
y = 0.0019x + 0.0443
R² = 0.85348

Figure 6

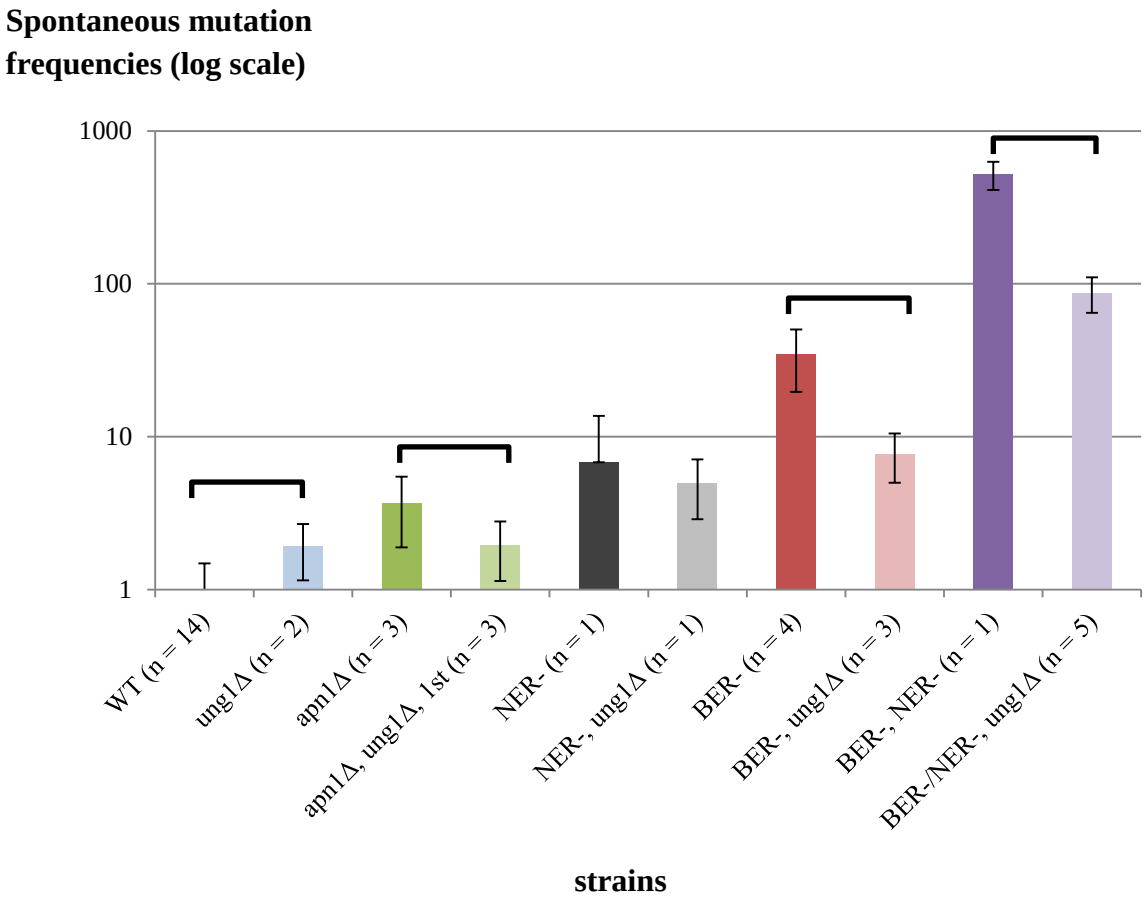
Spontaneous mutation frequencies (log scale)
1000
100
10
1
WT (n = 14)
ung1Δ (n = 2)
apn1Δ (n = 3)
apn1Δ, ung1Δ, 1st (n = 3)
NER- (n = 1)
NER-, ung1Δ (n = 1)
BER- (n = 4)
BER-, ung1Δ (n = 3)
BER-, NER- (n = 1)
BER-/NER-, ung1Δ (n = 5)
strains

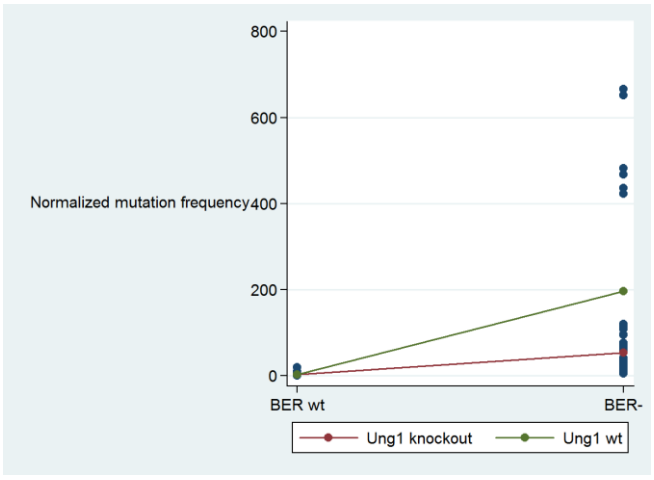
Normalized mutation frequency
800
600
400
200
0
BER wt
BER-
Ung1 knockout
Ung1 wt

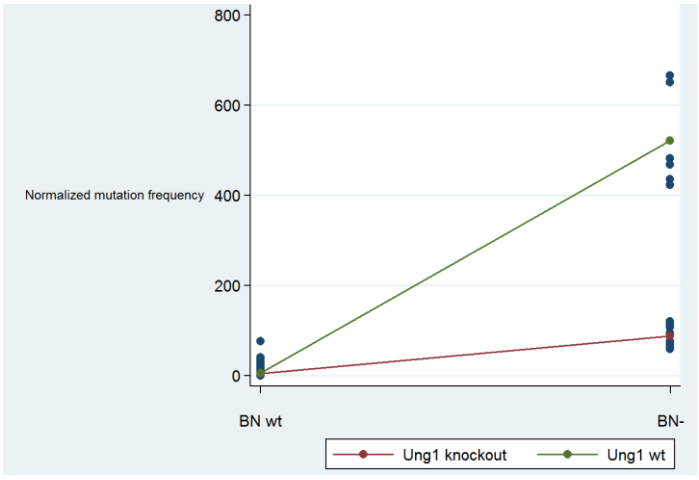
Normalized mutation frequency
800
600
400
200
0
BN wt
BN-
Ung1 knockout
Ung1 wt

Figure 7

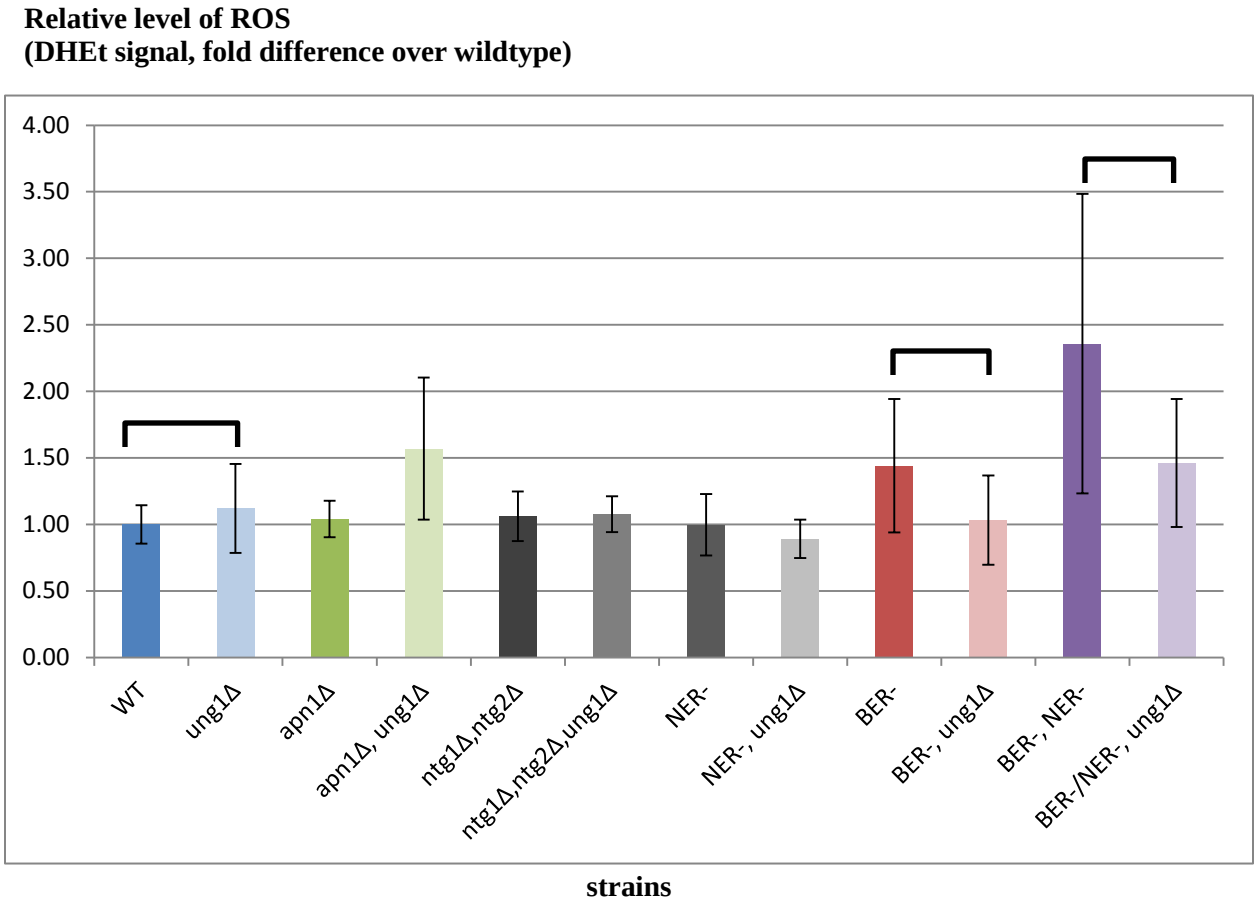
Relative level of ROS
(DHEt signal, fold difference over wildtype)
4.00
3.50
3.00
2.50
2.00
1.50
1.00
0.50
0.00
WT
ung1Δ
apn1Δ
apn1Δ, ung1Δ
ntg1Δ,ntg2Δ
ntg1Δ,ntg2Δ,ung1Δ
NER-
NER-, ung1Δ
BER-
BER-, ung1Δ
BER-, NER-
BER-/NER-, ung1Δ
strains

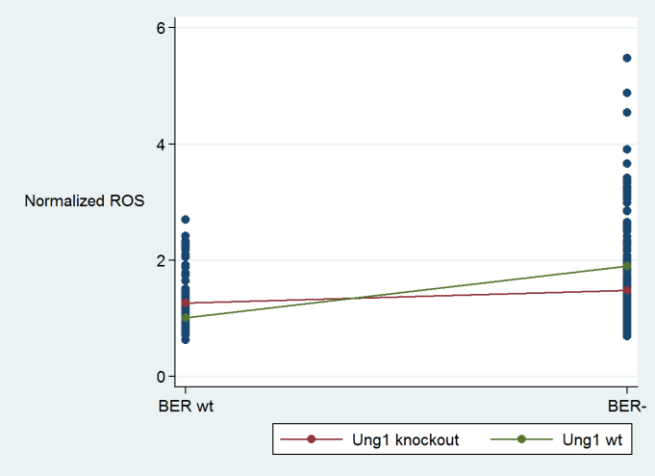
Normalized ROS
6
4
2
0
BER wt
BER-
Ung1 knockout
Ung1 wt

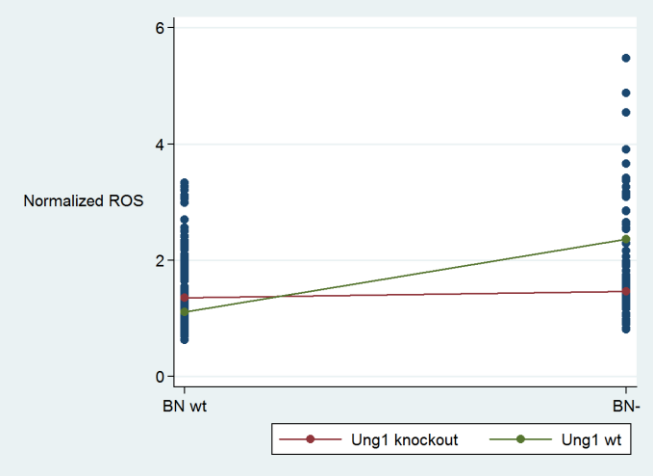
Normalized ROS
6
4
2
0
BN wt
BN-
Ung1 knockout
Ung1 wt

Figure 8

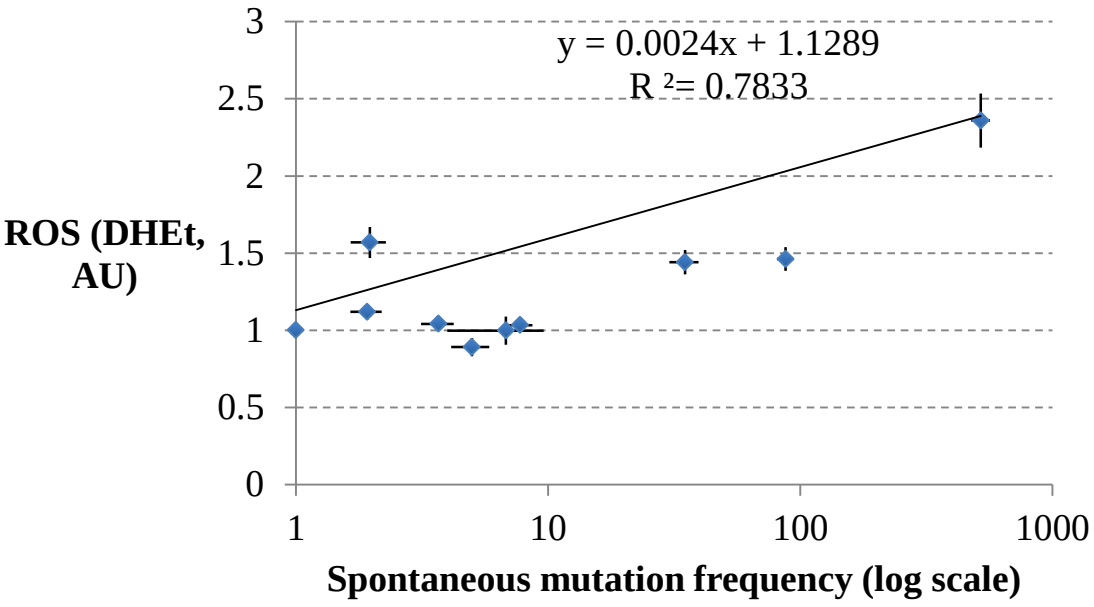
y = 0.0024x + 1.1289
R ²= 0.7833
ROS (DHEt, AU)
3
2.5
2
1.5
1
0.5
0
1
10
100
1000
Spontaneous mutation frequency (log scale)

Figure 9

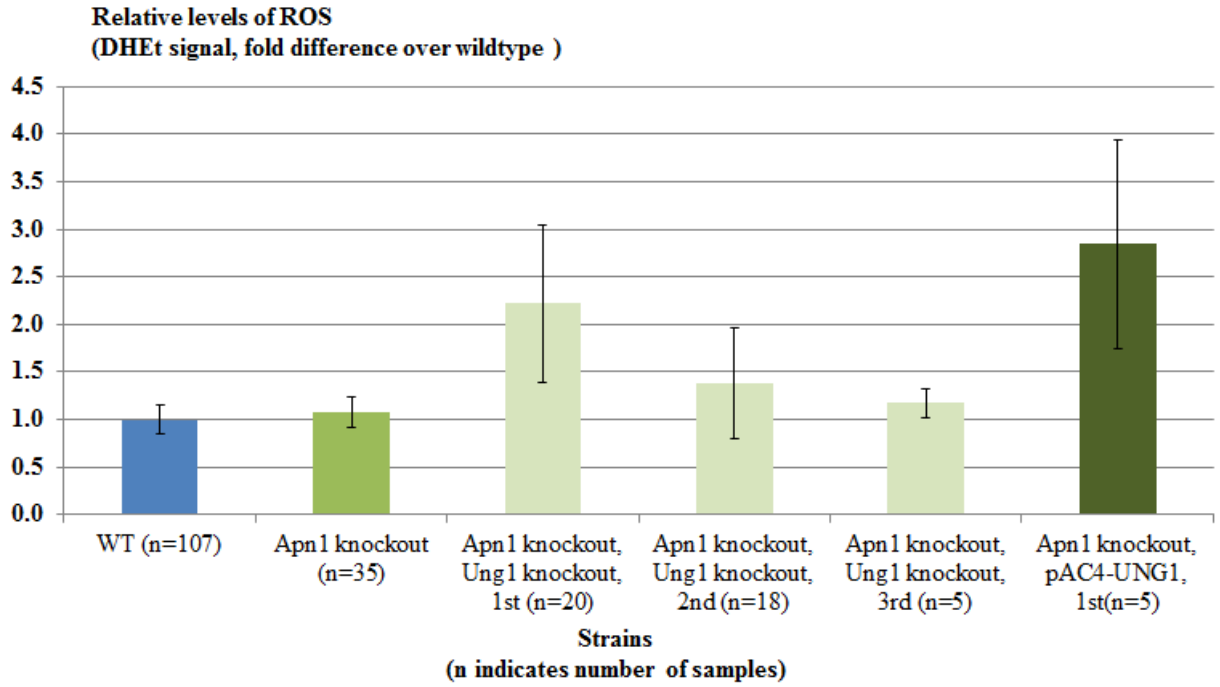
Relative levels of ROS
(DHEt signal, fold difference over wildtype )
4.5
4.0
3.5
3.0
2.5
2.0
1.5
1.0
0.5
0.0
WT (n=107)
Apn1 knockout (n=35)
Apn1 knockout, Ung1 knockout, 1st (n=20)
Apn1 knockout, Ung1 knockout, 2nd (n=18)
Apn1 knockout, Ung1 knockout, 3rd (n=5)
Apn1 knockout, pAC4-UNG1, 1st(n=5)
Strains
(n indicates number of samples)

Figure 10

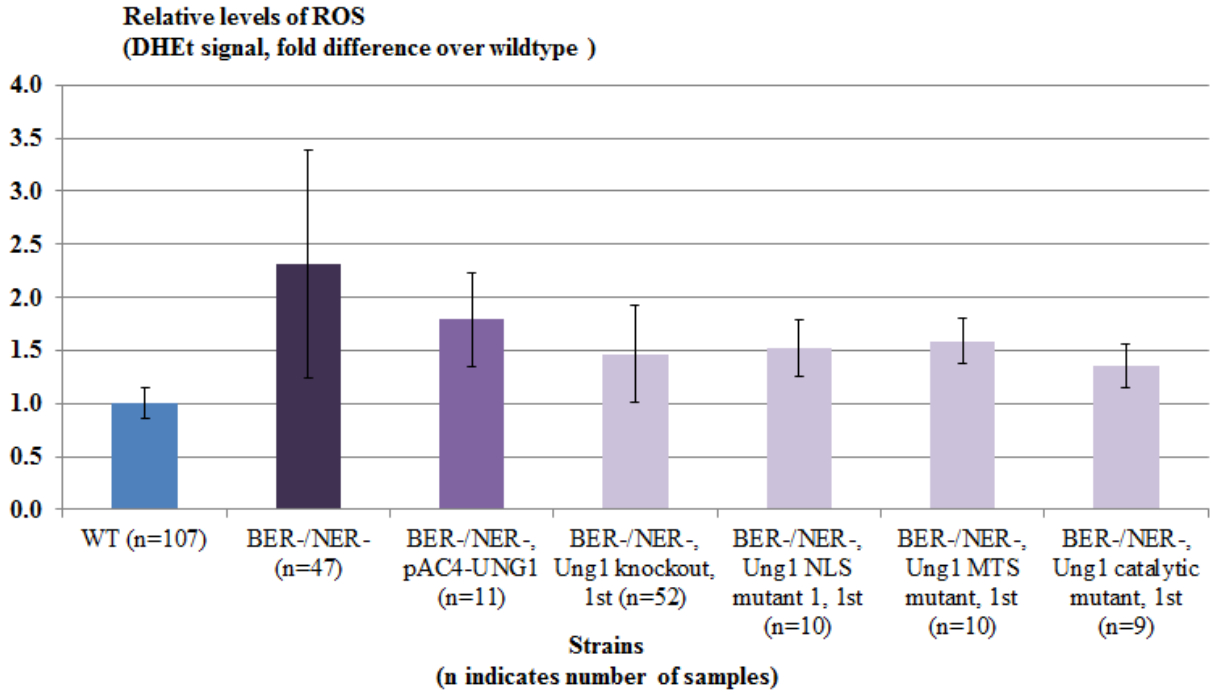
Relative levels of ROS
(DHEt signal, fold difference over wildtype )
4.0
3.5
3.0
2.5
2.0
1.5
1.0
0.5
0.0
WT (n=107)
BER-/NER- (n=47)
BER-/NER-, pAC4-UNG1 (n=11)
BER-/NER-, Ung1 knockout, 1st (n=52)
BER-/NER-, Ung1 NLS mutant 1, 1st (n=10)
BER-/NER-, Ung1 MTS mutant, 1st (n=10)
BER-/NER-, Ung1 catalytic mutant, 1st (n=9)
Strains
(n indicates number of samples)

Figure 11

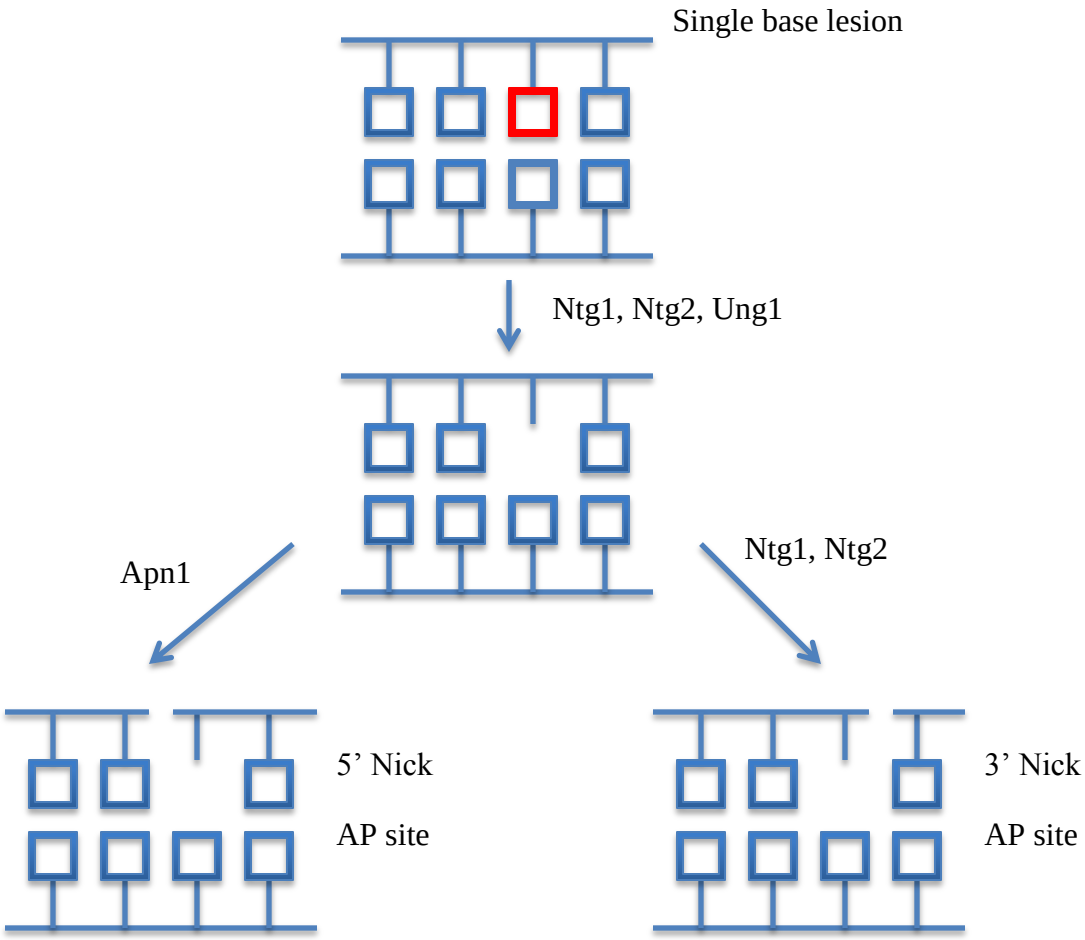
Single base lesion
Ntg1, Ntg2, Ung1
Apn1
Ntg1, Ntg2
5’ Nick
AP site
3’ Nick
AP site

# Tables

Table 1

| Strain/Plasmid | Genotype |
|---|---|
| hDNP119 (*6*) | *MAT***a**/*MAT*α *rad1*::*kanMX*/*RAD1 ntg1*::*hphMX4*/*NTG1 ntg2*::*BSD*/*NTG2 apn1*::*TRP1*/*APN1 dsf1*::*URA3*/*DSF1 his7-1*/*his7-1 lys2*Δ*5*'::*LEU-lys2*Δ*3*'/*lys2*Δ*5*'::*LEU-lys2*Δ*3*' *ade5-1*/*ade5-1 trp1-289*/*trp1-289 ura3-52*/*ura3-52 UNG1/ung1Δ::NAT* |
| WT | *MAT*α *his7-1 lys2*Δ*5*'::*LEU-lys2*Δ*3*' *ade5-1 trp1-289 ura3-52* |
| WT *ung1Δ* | WT *ung1Δ::NAT* |
| NER$^-$ | *MAT***a**[or]*MAT*α *rad1*::*kanMX his7-1 lys2*Δ*5*'::*LEU-lys2*Δ*3*' *ade5-1 trp1-289 ura3-52* |
| NER$^-$ *ung1Δ* | NER$^-$ *ung1Δ::NAT* |
| *apn1Δ* | *MAT***a**[or]*MAT*α *apn1*::*TRP1 his7-1 lys2*Δ*5*'::*LEU-lys2*Δ*3*' *ade5-1 trp1-289 ura3-52* |
| *apn1Δ, ung1Δ* | *apn1Δ ung1Δ::NAT* |
| *ntg1Δ, ntg2Δ* | *MAT***a**[or]*MAT*α *ntg1*::*hphMX4 ntg2*::*BSD his7-1 lys2*Δ*5*'::*LEU-lys2*Δ*3*' *ade5-1 trp1-289 ura3-52* |
| *ntg1Δ, ntg2Δ, ung1Δ* | *ntg1Δ ntg2Δ ung1Δ::NAT* |
| BER$^-$ | *MAT***a**[or]*MAT*α *ntg1*::*hphMX4 ntg2*::*BSD apn1*::*TRP1 his7-1 lys2*Δ*5*'::*LEU-lys2*Δ*3*' *ade5-1 trp1-289 ura3-52* |
| BER- *ung1Δ* | BER$^-$ *ung1Δ::NAT* |
| BER$^-$/NER$^-$ | *MAT***a**[or]*MAT*α *rad1::kanMX ntg1*::*hphMX4 ntg2*::*BSD apn1*::*TRP1 his7-1 lys2*Δ*5*'::*LEU-lys2*Δ*3*' *ade5-1 trp1-289 ura3-52* |
| BER$^-$/NER$^-$ *ung1Δ* | BER$^-$/NER$^-$ *ung1Δ::NAT* |
| DSC226 | *MATa ura3-52 leu2Δ1 his3Δ200* (*1*) |
| DSC499 | *MATa ura3-52 leu2Δ1 his3Δ200 ung1* |
| DSC500 | *MATa ura3-52 leu2Δ1 his3Δ200 ung1* p*UNG1*-GFP |

Table 1 (cont'd)

| | |
|---|---|
| pAC4-UNG1-GFP | *UNG1 URA3 Amp*$^r$ (pRS316 with yeast *CEN*) (*8*) |
| pAC4-*ung1*-GFP | *ung1-NLS URA3 Amp*$^r$ (nuclear localization sequence mutant)<br>*ung1-MTS URA3 Amp*$^r$ (mitochondria targeting sequence mutant)<br>*ung1-CataURA3 Amp*$^r$ ( catalytic mutant)<br>All inserts obtained from site-directed mutagenesis of *UNG1* (Doetsch lab, unpublished work) in strain DSC226 (*1*) |

Table 2

| Sample | Wells | Value | Average |
|---|---|---|---|
| BER- 0 mM MMS | D7 | 0.515 | |
| | D8 | 0.555 | |
| | D9 | 0.515 | 0.528 |
| BER- 25 mM MMS | F7 | 0.533 | |
| | F8 | 0.516 | |
| | F9 | 0.52 | 0.523 |
| WT 0 mM MMS | D2 | 0.584 | |
| | D3 | 0.552 | |
| | D4 | 0.554 | 0.563 |
| WT 25 mM MMS | F2 | 0.621 | |
| | F3 | 0.512 | |
| | F4 | 0.559 | 0.564 |

| Sample | Wells | Values | MeanValue |
|---|---|---|---|
| BER- $NaBH_4$ | B7 | 0.564 | 0.561 |
| | B8 | 0.552 | |
| | B9 | 0.566 | |
| WT $NaBH_4$ | B2 | 0.602 | 0.600 |
| | B3 | 0.61 | |
| | B4 | 0.589 | |

| | WT | $BER^-$ |
|---|---|---|
| 0 mM MMS | 0.563 | 0.528 |
| 25 mM MMS | 0.564 | 0.523 |
| $NaBH_4$-treated control | 0.600 | 0.561 |

Table 3

Dependent variable:
ROS level

Number of samples = 341

| Source | deg. of freedom | F value | p value |
|---|---|---|---|
| Model | 7 | 25.20 | 0.0000 |
| BER | 1 | 48.78 | 0.0000 |
| rad1 | 1 | 2.74 | 0.0989 |
| BER,rad1 interact. | 1 | 7.97 | 0.0050 |
| ung1 | 1 | 4.43 | 0.0361 |
| BER,ung1 interact. | 1 | 4.70 | 0.0309 |
| rad1,ung1 interact. | 1 | 8.97 | 0.0029 |
| BER,rad1,ung1 interact. | 1 | 3.41 | 0.0658 |

Dependent variable:
Mutation frequency

Number of samples = 119

| Source | deg. of freedom | F value | p value |
|---|---|---|---|
| Model | 7 | 358.35 | 0.0000 |
| BER | 1 | 713.03 | 0.0000 |
| rad1 | 1 | 587.83 | 0.0000 |
| BER,rad1 interact. | 1 | 552.18 | 0.0000 |
| ung1 | 1 | 374.14 | 0.0000 |
| BER,ung1 interact. | 1 | 371.23 | 0.0000 |
| rad1,ung1 interact. | 1 | 298.43 | 0.0000 |
| BER,rad1,ung1 interact. | 1 | 290.54 | 0.0000 |

## Figure and Table Legends

Figure 1. Model for the role of ROS in the genotoxic stress response

Figure 2. Top: partial amino acid sequence of yeast Ung1, showing putative NLS (highlighted in yellow), MTS (highlighted in cyan), aspartate in active site (in blue), and the mutations with which the localization/catalytic mutants are created. Bottom: plasmid map for Ung1 mutant-carrying pAC4.

Figure 3. Histograms from flow cytometry display greater peak values/approximate geometric means for dyed samples (right panel) and samples with more damage-prone genotype ($BER^-/NER^-$) (left panel).

Figure 4. MATLAB-generated distribution fits for flow cytometry histogram data (fluorescence in arbitrary units) in wildtype hDNP119 isolate sample following 2h incubation with 5μg/ml DHEt (fluorescence in arbitrary units).

Figure 5. Heating DNA negatively affects the aldehyde reactive probe (ARP) assay. Standard curves were generated from DNA standards provided from ARP kit (heated standards were subjected to 10min, 65℃ treatment, as DNA extraction required) in order to evaluate number of abasic sites present in DNA samples based on their OD values from the streptavidin-biotin photometric assay.

Figure 6. Top: Spontaneous mutation frequencies of hDNP119-derived strains with *UNG1* or *ung1Δ* based on numbers of canr mutations, with *apn1Δ*, $BER^-$ and $BER^-/NER^-$ isolates displaying reduced mutagenesis. (Brackets indicate statistical significance: $p<0.05$, ANOVA. n indicates number of assays, 4-6 samples per assay, error determined via standard deviation.) Bottom: ANOVA plots showing the predicted means for $BER^-$ and $BER^-/NER^-$ with/without Ung1. The effects of $BER^-$ and $BER^-/NER^-$ are dampened by *ung1Δ*. (Blue dots indicate data distribution; "BN-" stands for $BER^-/NER^-$.)

Figure 7. Top: Intracellular ROS levels of above isolates based on DHEt signal measured via flow cytometry, with a clear reduction for (two out of three) BER- and BER-/NER- background ung1Δ isolates. Brackets indicate statistical significance (brackets indicate statistical significance: $p<0.05$, ANOVA. 1st/2nd/3rd marks isolates of the same background from different dissections, n indicates number of trials, 4-6 samples per trial, error determined via standard deviation). Bottom: ANOVA plots showing the predicted means for $BER^-$ and $BER^-/NER^-$ with/without Ung1. The effects of $BER^-$ and $BER^-/NER^-$ are dampened by *ung1Δ*. (Blue dots indicate data distribution; "BN-" stands for $BER^-/NER^-$.)

Figure 8. Correlation between spontaneous mutation frequency and ROS level (in arbitrary units), both normalized to WT, fitted to a linear model (error determined via standard error of the mean).

Figure 9. hDNP119 isolate (*apn1Δ, ung1Δ*) transformed with pAC4-*UNG1*-GFP shows increased level of ROS generation over both *apn1Δ* and *apn1Δ, ung1Δ* isolates (n indicates number of samples, error determined via standard deviation; relationships among all isolates are significant by *t*-test).

Figure 10. Intracellular ROS levels of $BER^-/NER^-$, *ung1Δ* transformants carrying *CEN* plasmid (pAC4) with *UNG1* or its localization/catalytic function mutant inserts, based on DHEt signal measured via flow cytometry. Neither nuclear nor mitochondrial targeting mutants display significant change from the Ung1 knockout. (Relationships between all strains are significant by Student's *t*-test, $p<0.05$. n indicates number of samples, error determined via standard deviation).

Figure 11. Partial diagram of yeast base excision repair pathway, showing the enzymes involved in this study. Removal of a DNA lesion (denoted by the red square) in step 1 via glycosylase function results in the formation of an abasic site.

Table 1. Strains and plasmids used in this study and their genotypes.

Table 2. ARP assay microtiter plate data from hDNP119 WT and $BER^-$ isolates, fourth trial, with 0mM/25mM MMS treatment and $NaBH_4$-treated controls. No significant difference was seen between 0mM and 25mM MMS treated samples, and $NaBH_4$ treatment control signals greater than both WT and $BER^-$ samples were obtained.

Table 3. Top: three-way ANOVA of ROS levels by BER, NER (*rad1 Δ*), and Ung1 status (presence/absence), with all interactions/effects of ROS level (except NER alone and three-way) significant (p values less than 0.05). Bottom: three-way ANOVA of mutation frequencies by BER, NER, and Ung1 status. All interactions/effects are significant.

## References


1. L.A. Rowe, N. Degtyareva, P.W. Doetsch, DNA damage-induced reactive oxygen species (ROS) stress response in *Saccharomyces cerevisiae*. Free Radical Biology and Medicine 45 (2008) 1167-1177
2. M. Guillet, S. Boiteux, Origin of endogenous DNA abasic sites in *Saccharomyces Cerevisiae*. Molecular Cellular Biology 23 (2003) 8386-8394
3. R.T. Elder, X. Zhu, S. Priet, M. Chen, M. Yu, J.M. Navarro, J. Sire, Y. Zhao, A fission yeast homologue of the human uracil-DNA-glycosylase and their roles in causing DNA damage after overexpression. Biochemical and Biophysical Research Communications 306 (2003) 693-700
4. S.L. Yu, S.K. Lee, R.E. Johnson, L. Prakash, S. Prakash, The stalling of transcription at abasic sites is highly mutagenic. Molecular Cellular Biology 23 (2003) 382-388
5. L.M. Griffiths, D. Swartzlander, K.L. Meadows, K.D. Wilkinson, A.H. Corbett, P.W. Doetsch, Dynamic Compartmentalization of Base Excision Repair Proteins in Response to Nuclear and Mitochondrial Oxidative Stress. Molecular Cellular Biology 29 (2009) 794-807
6. N.P. Degtyareva, L. Chen, P. Mieczkowski, T.D. Petes, P.W. Doetsch, Chronic oxidative DNA damage due to DNA repair defects causes chromosomal instability in *Saccharomyces cerevisiae*. Molecular Cellular Biology 28 (2008) 5432-5445
7. D.X. Tishkoff, N. Filosi, G.M. Gaida, R.D. Kolodner, A novel mutation avoidance mechanism dependent on *S. cerevisiae RAD27* is distinct from DNA mismatch repair. Cell 88 (1997) 253-263
8. R.S. Sikorski, P. Hieter, A system of shuttle vectors and yeast host strains designed for efficient manipulation of DNA in *Saccharomyces cerevisiae*. Genetics 122 (1989) 19-27
9. A.M. Wilstermann, N. Osheroff, Base excision repair intermediates as topoisomerase II poisons. Journal of Biological Chemistry 276 (2001) 46290-46296
10. L. Eckhard, W.A. Stahel, M. Abbt, Log-normal distributions across the sciences: keys and clues. BioScience 51 (2001) 341-352
11. E.C. Friedberg, DNA damage and repair. Nature 421 (2003) 436-440
12. J. Nakamura and J.A. Swenberg, Endogenous apurinic/apyrimidinic sites in genomic DNA of mammalian tissues. Cancer Research 59 (1999) 2522-2526
13. S.E. Tsutakawa, D.S. Shin, C.D. Mol, T. Izumi, A.S. Arvai, A.K. Mantha, B. Szczesny, I.N. Ivanov, D.J. Hosfield, B.Maiti, M.E. Pique, K.A. Frankel, K. Hitomi, R.P. Cunningham, S. Mitra, J.A. Tainer, Conserved structural chemistry for incision activity in structurally non-homologous apurinic/apyrimidinic endonuclease APE1 and endonuclease IV DNA repair enzymes. Journal of Biological Chemistry Papers in Press (2013) M112.422774
14. S.D. Markowitz, M.M. Bertagnolli, Molecular origins of cancer: molecular basis of colorectal cancer. New England Journal of Medicine 361 (2009) 2449–2460

15. A. Karalis. M. Tischkowitz, G.W. Millington, Dermatological manifestations of inherited cancer syndromes in children. British Journal of Dermatology 164 (2011) 245-256
16. T. Finkel, N.J. Holbrook, Oxidants, oxidative stress and the biology of ageing. Nature 408 (2000) 239-247
17. J.H. Hoejmakers, Genome maintenance mechanisms for preventing cancer. Nature 411 (2001) 366-374
18. M. Genestra, Oxyl radicals, redox-sensitive signaling cascades and antioxidants. Cellular Signaling 19 (2007) 1807-1819
19. S. Boiteux, M. Guillet, Use of yeast for detection of endogenous abasic site lesions, their source, and their repair. Methods in Enzymology 408 (2006) 79-91
20. K.W. Steen, B. Doseth, M.P. Westbye, M. Akbari, D. Kang, M. Falkenberg, G. Slupphaug, mtSSB may sequester UNG1 at mitochondrial ssDNA and delay uracil processing until the dsDNA conformation is restored. DNA Repair 11 (2012) 82-91
21. C.Y. Chien, C.K. Chou, J.Y. Su, Ung1p-mediated uracil-base excision repair in mitochondria is responsible for the petite formation in thymidylate deficient yeast. FEBS Letters 583 (2009) 1499-1504
22. D.B. Swartzlander, L.M. Griffiths, J. Lee, N.P. Degtyareva, P.W. Doetsch, A.H. Corbett, Regulation of base excision repair: Ntg1 nuclear and mitochondrial dynamic localization in response to genotoxic stress. Nucleic Acids Research 38 (2010) 3963-3974
23. B.M. Babior, NADPH oxidase: an update. Blood 93 (1999) 1464-1476
24. Y. Qian, C. Wei, F.E. Lee, J. Campbell, J. Halliley, J.A. Lee, J. Cai, Y.M. Kong, E. Sadat, E. Thomson, P. Dunn, A.C. Seegmiller, N.J. Karandikar, C.M. Tipton, T. Mosmann, I. Sanz, R.H. Scheuermann, Elucidation of seventeen human peripheral blood B-cell subsets and quantification of the tetanus response using a density-based method for the automated identification of cell populations in multidimensional flow cytometry data. Clinical Cytometry 78B (2010) S69-S82
25. S. Yu, X. Zhang, G. Chen, W. Liu, Compromised cellular responses to DNA damage accelerate chronological aging by incurring cell wall fragility in *Saccharoyces cerevisiae*. Molecular Biology Reports 39 (2012) 3573-3583
26. I. Peluso, G. Adorno, A. Raguzzini, L. Urban, A. Ghiselli, M. Serafini, A new flow cytometry method to measure oxidative status: The Peroxidation of Leukocytes Index Ratio (PLIR). Journal of Immunological Methods 390 (2013) 113-120
27. C.L. Chan, L. Rénia, K.S. Tan, A simplified, sensitive phagocytic assay for malaria cultures facilitated by flow cytometry of differentially-stained cell populations. PLoS One 7 (2012) e38523
28. D.M. Zhou, Q. Xi, M.F. Liang, C.H. Chen, L.J. Tang, J.H. Jiang, Graphene oxide-hairpin probe nanocomposite as a homogeneous assay platform for DNA base excision repair screening. Biosensors and Bioelectronics 41 (2013) 359-365

29. K.P. Roberts, J.A. Sobrino, J. Payton, L.B. Mason, R.J. Turesky, Determination of apurinic/apyrimidinic lesions in DNA with high-performance liquid chromatography and tandem mass spectrometry. Chemical Research in Toxicology 19 (2006) 300-309
30. Y. Wang, L. Liu, C. Wu, A. Bulgar, E. Somoza, W. Zhu, S.L. Gerson, Direct detection and quantification of abasic sites for in vivo studies of DNA damage and repair. Nuclear Medicine and Biology 36 (2009) 975-983
31. S. Lari, C. Chen, B.G. Vertéssy, J. Morré, S.E. Bennett, Quantative determination of uracil residues in *Escherichia coli* DNA: contribution of *ung*, *dug*, and *dut* genes to uracil avoidance. DNA Repair 5 (2006) 1407-1420
32. Y.W. Kow, A. Dare, Detection of abasic sites and oxidative DNA base damage using an ELISA-like assay. Methods 22 (2000) 164-169
33. N. Haruta, Y. Kubota, T. Hishida, Chronic low-dose ultraviolet-induced mutagenesis in nucleotide excision repair-deficient cells. Nucleic Acids Research 40 (2012) 8406-8415
34. B.L. Tallec, A. Peyroche, Using DNA damage sensitivity phenotypes to characterize mutations affecting proteasome function. Methods in Molecular Biology 832 (2012) 363-371
35. P. Auerbach, R.A.O. Bennett, E.A. Bailey, H.E. Krokan, B. Demple, Mutagenic specificity of endogenously generated abasic sites in *Saccharomyces cerevisiae* chromosomal DNA. PNAS 102 (2005) 17711-17716
36. H. Sugiyama, T. Fujiwara, A. Ura, T. Tashiro, K. Yamamoto, S. Kawanishi, I. Saito, Chemistry of thermal degradation of abasic sites in DNA: mechanistic investigation on thermal DNA strand cleavage of alkylated DNA. Chemical Research in Toxicology 7 (1994) 673-683
37. C.A. Hendricks, M. Razlog, T. Matsuguchi, A. Goyal, A.L. Brock, B.P. Engelward, The *S. cerevisiae* Mag1, 3-methyladenine DNA glycosylase modulates susceptibility to homologous recombination. DNA Repair 1 (2002) 645-659
38. B. Kayli, G. Slupphaug, C.D. Mol, A.S. Arvai, S.B. Peterson, J.A. Tainer, H.E. Krokan, Excision of cytosine and thymine from DNA by mutants of human uracil-DNA glycosylase. The EMBO Journal 15 (1996) 3442-3447
39. A.J. Stevens, L. Guan, K. Bebenek, T.A. Kunkel, M.M. Greenberg, DNA polymerase λ inactivation by oxidized abasic sites. Biochemistry 52 (2013) 975-983
40. A. Chatterjee, K.K. Singh, Uracil-DNA glycosylase-deficient yeast exhibit a mitochondrial mutator phenotype. Nucleic Acids Research 29 (2001) 4935-4940